Probabilistic demand assessment of bridges considering the effect of corrosion and seismic loading over time

Dante Tolentino (dantetl@azc.uam.mx)
Universidad Autonoma Metropolitana https://orcid.org/0000-0003-3930-3562
Daniel Herrera
Universidad Autonoma Metropolitana
Ricardo B. Flores
Universidad Autonoma Metropolitana

Research Article

Keywords: corrosion effect, cumulative damage, fragility curves, demand hazard curves, bridges.

Posted Date: June 9th, 2021

DOI: https://doi.org/10.21203/rs.3.rs-598775/v1

Probabilistic demand assessment of bridges considering the effect of corrosion and seismic loading over time

Dante Tolentino[1*], Daniel Herrera[1], Ricardo B. Flores[1]

(1) Departamento de materiales, Universidad Autónoma Metropolitana, CDMX 02200, México

dantetl@azc.uam.mx; al2203801952@azc.uam.mx; al2182800042@azc.uam.mx

*Corresponding author: dantetl@azc.uam.mx

Abstract

This paper proposes an approach to calculate demand hazard curves considering the effect of both corrosion and seismic loadings over time. The corrosion is defined as the reduction of the cross-sectional area in the reinforced bars of concrete, induced by chloride ions. Three corrosion phases are considered: starting time of corrosion, cracking, and evolution time. Seismic loads are characterized as a stochastic Poisson process. Uncertainties related to the randomness of geometric properties, mechanical properties, and seismic loadings are considered. The approach is illustrated in a continuous bridge designed to comply with a drift of 0.002. The structure is located in Acapulco, Guerrero, Mexico. Fragility curves and demand hazard curves are obtained at 0, 45, 57, 75, 100, and 125 years, based on the global drift. The effect of both corrosion and seismic loadings over time increase the annual rate of demand up to 308% between 0 years (without damage) and 125 years after the bridge construction.

Keywords: corrosion effect, cumulative damage, fragility curves, demand hazard curves, bridges.

1 Introduction

Corrosion in reinforced concrete structures is an influential phenomenon, particularly in structures located near coastal areas. Such phenomenon is frequently present in structures exposed to weathering, which creates a tough environmental condition when sea breeze acts. The particles of chloride ions that come from the sea hit the surface of the bridge, until the amount of such particles is enough to permeate through the concrete, eventually reaching the reinforcement steel, starting both the corrosion process and the structural deterioration.

Corrosion has an economic and social impact: in The United States, it represents losses which are around 4.9% of the Gross Domestic Product (GDP) of that country, according to studies by the US National Bureau of Standards (NBS) (Schwerdtfeger et al. 1972). In Mexico, there are no precise statistics, but if a similar percentage is considered, the impact of corrosion in Mexico results in US$ 38 billion, according to data of the National Institute of Statistics and Geography (INEGI 2018) for 2018. Approaches to estimate the vulnerability of structures that would allow making repair and maintenance decisions with the aim to reduce the cost that produces the effect of corrosion are necessary.

Several authors have studied the effect of corrosion: Andrade et al. (1993) used micrometers to register visible corrosion cracking in structural elements; Mangat and Molloy (1994) demonstrated that the diffusion coefficient can be associated with both the time interval of the concrete exposure to chloride and the Fick's second law that reproduces the corrosion diffusion into structural components; Cabrera (1996) determined that corrosion can move through parallel cracking into reinforcement steel; Thoft-Christensen (2000) proposes a stochastic model for structural reliability assessment based on the cracking width caused by corrosion; Thoft-Christensen (2002) gives a methodology for the evaluation of structural reliability in reinforced concrete structures showing different phases of corrosion; Thoft-Christensen (2003) presents a stochastic model to estimate the diffusion coefficient; Bertolini (2008) shows that the steel bars of reinforced concrete are protected

by an alkaline solution that is inside of a hydrated cement paste; Jaffer and Hansson (2009) studies the distribution of corrosion formed in cracked reinforced concrete; lastly, Papakonstantinou and Shinozuka (2013) propose an approach to simulate corrosion over time in concrete structures.

Two codes are mainly used for the design of bridges in Mexico: the code of the Mexican Institute of Transportation (IMT 2004) and the code of the American Association of State Highways (AASHTO 2012). When the IMT code is used, the last stages of structural design are done using other codes, because such code is incomplete. Therefore, uncertainties related to the characterization of loads and mechanical properties are generated. Mexico has experienced important economic losses, especially with the earthquakes occurred in 1985 and 2017: such events generated a loss of 9.2 billion dollars.

Considering that bridge structures can present structural damage after seismic loading, some authors propose methodologies to estimate safety levels in bridges expressed in terms of fragility curves: Choi and Jeon (2003) evaluates the fragility of bridges and retrofit measures to increase the seismic resistance of the bridge structures; Kim and Feng (2003) estimates fragility curves considering different intensity measures; fragility curves are calculated in different kinds of bridges and zones in the United States (Choi et al. 2004; Pan et al. 2007); analytical fragility analysis is proposed for different components of the bridge structure (Padgett and DesRoches 2008). Wang et al. (2012) estimates fragility curves considering multidimensional performance limit state parameters in concrete bridges; a multivariate fragility analysis is made considering the uncertainties in the seismic loadings (Wang et al. 2018); the effect of the cumulative damage by seismic loadings is taken into account in the fragility analysis (Cui et al. 2019; Panchireddi and Ghosh 2019; Tolentino et al. 2020). Fragility curves have been used in different approaches as the basis for obtaining exceedance damage rates or probabilistic demand hazard curves: Mackie and Stojadinović (2001) evaluates the seismic demand analysis in typical bridges located in California; Gavabar and Alembagheri (2018) proposes a methodology to estimate

seismic demand hazard curves in gravity dams; probabilistic demand hazard curves are estimated in concrete buildings (Liu et al. 2016), in steel buildings with different types of connections (Maleki et al. 2019), in steel buildings with buckling-restrained braces (Mahdavipour 2016; Afsar Dizaj et al. 2018), and in steel buildings with butterfly-shaped fuses (Zaker Esteghamati and Farzampour, 2020).

An approach for evaluating demand hazard curves considering both the cumulative damage under seismic sequences and the effect of corrosion over time has never been done. In this study, fragility curves over time are estimated for different time thresholds, considering both the effect of corrosion and seismic sequences at different instants of time. After fragility estimation, seismic demand hazard curves are calculated. The approach is exemplified in a reinforcement concrete bridge designed to comply with a drift of 0.002.

2 Probabilistic approach

2.1 Probabilistic demand assessment over time

The demand hazard curve, $v_D(d)$, can be obtained as follows (Cornell et al. 2002):

$$v_D(d) = \int_0^\infty \left|\frac{dv(y)}{dy}\right| P(D \geq d_{th}) dy \quad (1)$$

where $dv(y)/dy$ represents the derivative of the seismic annual rate of failure, and $P(D \geq d_{th})$ is the probability that the demand D exceeds a pre-established damage threshold d. If uncertainties in the structural demand are considered, the mean annual demand rate can be estimated as follows:

$$v_D(d) = \int_0^\infty \int_0^\infty \left|\frac{dv(y)}{dy}\right| P(D \geq d_{th}|y,d) f_d(d) dy dd \quad (2)$$

where $P(D \geq d_{th}|y,d)$ is the probability that a certain damage threshold is exceeded for a given intensity y. Considering both the variation in the structural demand and its probability density function given by corrosion at instant t, the exceedance rate of the demand at an instant t is as follows:

$$v_D(d,t) = \int_0^t \int_0^\infty \int_0^\infty \left|\frac{dv(y)}{dy}\right| P(D_{corr}(t) \geq d|y,t) f_{D_{corr}}(d|t) dy dd dt \quad (3)$$

where $P(D_{corr}(t) \geq d_{th}|y,t)$ is the probability that the structural demand due to corrosion results greater than a pre-established value of d_{th} for an intensity y at instant t, and $f_{D_{corr}}(d|t)$ is the probability density function of the seismic demand due to a state of corrosion at instant, t; it is shown that $v_D(d,t)$ is equal to $v_D(d)$ when $t = 1$.

2.2 Corrosion process in reinforced concrete

The corrosion in reinforced concrete systems appears given by the alkalinity generated by the accumulation of the passive layer in steel. In case of structures near marine environments, chloride ions penetrate the pores of concrete, until they reach the reinforcement steel. Therefore, the passive layer is removed, causing the beginning of corrosion.

2.2.1 Corrosion induced by chloride penetration

The effect of the corrosion in concrete structures by chloride penetration is not easy to characterize; it is commonly assumed that chloride ions follow the Fick's Law (Fick 1855). If the diffusion coefficient is considered as independent and the concentration of chlorides on the concrete surface is regarded as critical, the following expression can be generated:

$$\frac{\partial C(x,t)}{\partial t} = D_c \frac{\partial^2 C(x,t)}{\partial x^2} \quad (4)$$

where $C(x,t)$ represents the concentration of chloride ions as a percentage of the concrete weight at a certain distance x of the concrete surface at instant t; D_c is the diffusion coefficient. If the critical concentration of chlorides C_{cr} on the structural element is reached, the time that chloride ions take to reach the steel reinforcement can be determined by the following expression:

$$T_{corr} = \frac{d^2}{4D_c}\left[erf^{-1}\left(\frac{C_{cr}-C_0}{C_i-C_0}\right)\right]^{-2} \quad (5)$$

where T_{corr} is the starting time of corrosion, C_{cr} is the critical ions concentration, C_i is chloride concentration at the starting time of corrosion, and C_0 is the chloride concentration in the exposed zone of concrete. Such concentrations are all expressed in terms of a percentage of the concrete weight. erf is the error function, and d is the coating. The diffusion coefficient D_c, is estimated as follows:

$$D_c = 11.146 - 31.025\left(\frac{w}{c}\right) - 1.941\phi + 38.212\left(\frac{w}{c}\right)^2 + 4.48\left(\frac{w}{c}\right)\phi + 0.024\phi^2 \quad (6)$$

where w/c represents the relationship between the water and cement, and ϕ is the temperature.

2.2.1 Corrosion over time

The diameter reduction of steel reinforcement is estimated as follows (Thoft-Christensen 2002):

$$d(t) = d_0 - c_{corr} i_{corr}(t - T_{corr}) \qquad t \geq T_{corr} \quad (7)$$

where $d(t)$ is the reduced diameter at instant t, d_0 is the diameter that results from the design, i_{corr} is the corrosion mean annual rate, and C_{corr} is the coefficient of corrosion.

2.2.1 Corrosion over time

The instant of concrete cracking can be estimated as follows (Liu and Weyers 1998; Thoft-Christensen 2000):

$$\Delta t_{crack} = \frac{{W_{crit}}^2}{2k_{rust}} \tag{8}$$

where W_{crit} is the necessary amount of rust to induce cracking; k_{rust} is a proportional factor of i_{corr}. W_{crit} and k_{rust} can be calculated as follows:

$$W_{crit} = W_{steel}(W_{expan} + W_{porous}) \tag{9}$$

$$k_{rust} = 7.039E-05\frac{\pi d_0 i_{corr}}{\alpha} \tag{10}$$

where W_{expan} is the required amount of corrosion to replace the area as a consequence of concrete expansion; W_{steel} is the necessary amount of rust to generate cracking; W_{porous} is the volume of rust needed to fill a pore. W_{expan} and W_{steel} are calculated as follows:

$$W_{steel} = \frac{\rho_{steel}}{\rho_{steel} - \alpha\rho_{rust}} \tag{11}$$

$$W_{expan} = \pi\rho_{rust}t_{crit}\left(d_0 + 2t_{pore}\right) \tag{12}$$

where ρ_{steel} is the steel density; ρ_{rust} represent the rust density; $\alpha = 0.57$ (Liu and Weyers 1998); t_{crit} represent the thickness at the moment when the fracture beginning and it is estimated as (Liu and Weyers 1998):

$$t_{crit} = \frac{df_t}{E_c}\left(b\frac{a^2+b^2}{b^2-a^2} + \nu_c\right) \quad (13)$$

where E_c is the elasticity modulus, f_t is the concrete tensile strength, and ν_c is the Poisson ratio. Parameters a and b are estimated as follows (Thoft-Christensen 2002):

$$a = \frac{d_0+2t_{pore}}{2} \quad (14)$$

$$b = d + \left(\frac{d_0+2t_{pore}}{2}\right) \quad (15)$$

where a is the width of the steel rod, b is the distance between the centroid of the steel rod and the coating, and t_{pore} is the thickness that is similar to a value of porosity equal to 1. Once the cross-sectional area begins to degrade, a rust layer is generated around the reinforcing steel. When such rust reaches a critical amount, it generates additional stresses in the concrete that cause it to crack. Thoft-Christensen (2002) proposes an expression to determine the amount of rust W_{porous} as follows:

$$W_{porous} = t_{pore}\,\pi\rho_{rust}d_0 \quad (16)$$

2.3 Intensities and waiting times

Intensities and waiting times are simulated using the seismic hazard curve SHC, which is considered as a known variable associated with the fundamental period T. A critical damping equal to 5% is assumed. The simulation of intensities is based on the cumulate distribution function (CDF) of the SHC, as follows:

$$F(y) = 1 - \frac{\mathrm{SHC}_{fit}}{v_0} \tag{17}$$

where $\mathrm{SHC}_{fit} = \left(\frac{y}{y_0}\right)^{-r}\left(\frac{y_{max}-y}{y_{max}-y_0}\right)^{\varepsilon}$ is the expression that fitted the SHC, and y_0 is the seismic intensity necessary to produce structural damage in the structure. In this particular case, $y_0 = 1\ \mathrm{m/s^2}$, which is associated with an exceedance rate equal to $v_0 = 0.07737$. $y_{máx}$ represents the maximum value of seismic intensity in the SHC, r and ε are adjustment constants, and y represents all possible seismic intensities in the SHC.

The arrival of earthquakes can be characterized as a stochastic Poisson process. Therefore, the arrival time between earthquakes can be characterized by an exponential distribution function (Melchers and Beck 2017). Making some arrangements, the waiting time between seismic occurrences T_i is:

$$T_i = -\left|\frac{ln(u)}{v_0}\right| \tag{18}$$

where u represents random numbers between 0 and 1 with uniform distribution.

3 Cumulative damage assessment

Cumulative damage assessment is done based on the assumptions related with the type of structure, loadings, and the existence of a maintenance plan. In this study, the structure is subjected to seismic loadings and corrosion; no maintenance actions are made after loadings. The damage that the structure can gradually accumulate is estimated considering the simulation of seismic intensities and waiting times, as well as the different times related with the corrosion process. The cumulative process of damage is described in Fig. 1.

4 Illustrative example

Demand hazard curves are estimated considering different instants between the range of 0 to 125 years. The approach is illustrated in a typical reinforced concrete bridge designed to comply with a drift threshold of 0.002. The structure has a four-lane roadway, a total length of 175 m, and a height clearance of 8 m. For analysis and design purposes, the following conditions are taken into consideration: concrete in cap beams and columns has a compressive strength $f'c$ of 29.42 MPa; concrete in AASHTO-type beams has a compressive strength $f'c$ of 39.23 MPa; the supports in columns are fixed; there is an elastic spring with infinite stiffness in both directions between beams and cap beams; the extreme spans of the bridge have seat-type abutments; the period of vibration of the system is 0.40 s; the bridge is located in Acapulco, Mexico. Fig. 2 shows the transverse view of the structure, Fig. 3 shows the longitudinal view, and Fig. 4 shows the geometry and the design of cap beams and columns.

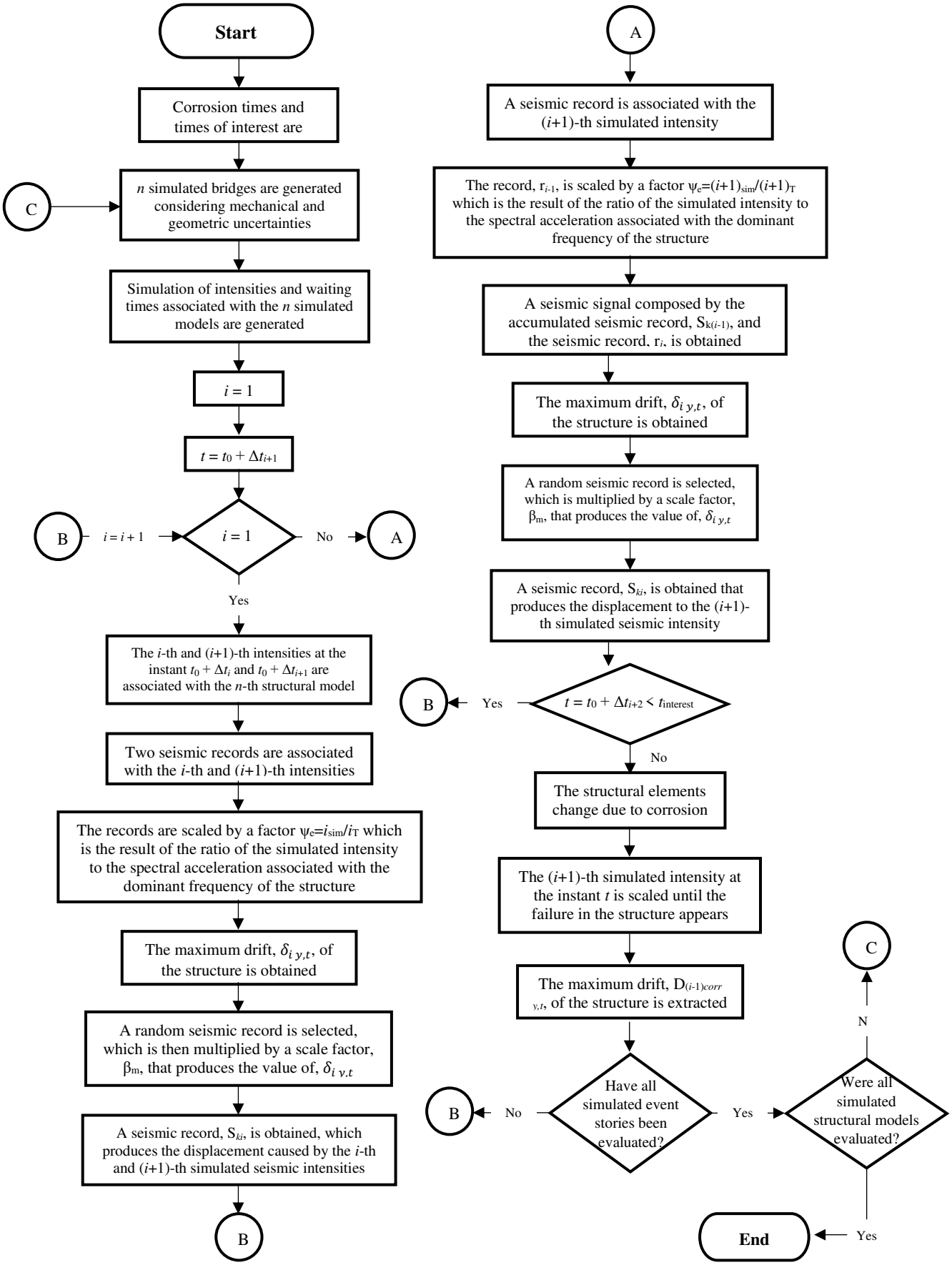

Fig. 1 Cumulative damage process

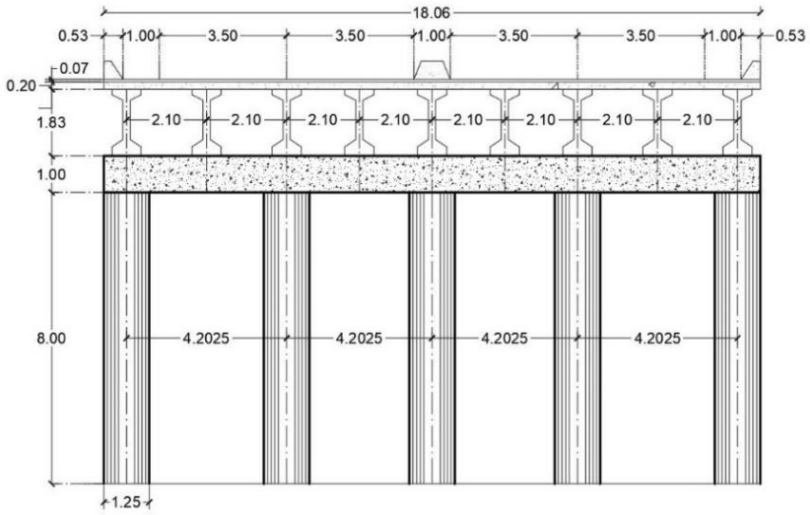

Fig. 2 Transverse view

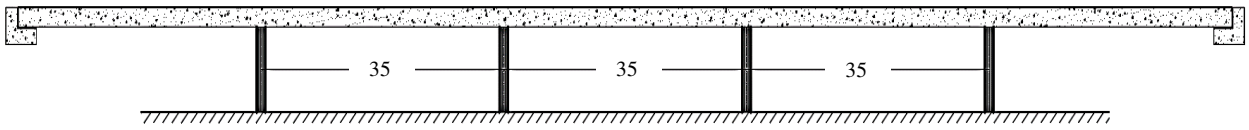

Fig. 3 Longitudinal view

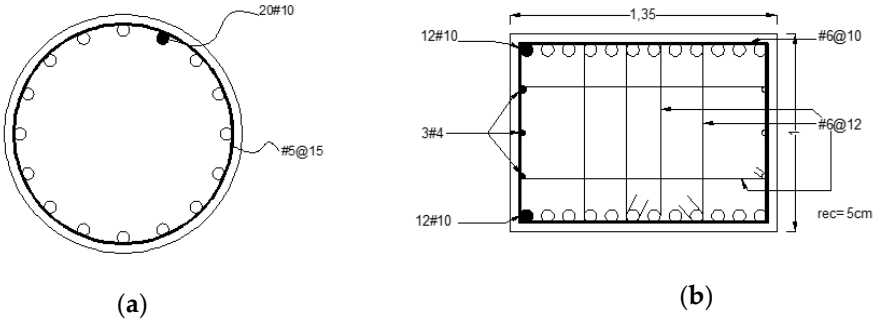

Fig. 4 Geometry and design of: (a) Columns; (b) Cap beams

4.1 Uncertainties in mechanical and geometric properties

The uncertainties associated with mechanical and geometric characteristics are essential parameters to assess the structural fragility with the aim to estimate demand hazard curves. Thus, Table 1 shows the mechanical uncertainties and Table 2 shows the geometric uncertainties considered in this study.

Table 1 Mechanical uncertainties.

Element	Variable	Bias factor, λ	Coefficient of variation, V	Reference
Columns, Beam Caps and Slab	f'c (MPa)	1.27	0.160	(Nowak et al. 2011)
AASHTO beams	f'c (MPa)	1.16	0.127	(Nowak et al. 2011)
Steel diameter #≤1/2	fy (MPa)	1.097	0.081	(Rodríguez and Botero 1995)
Steel diameter #>1/2	fy (MPa)	1.068	0.037	(Rodríguez and Botero 1995)
Steel diameter #≤1/2	fu (MPa)	1.180	0.039	(Rodríguez and Botero 1995)
Steel diameter #>1/2	fu (MPa)	1.155	0.022	(Rodríguez and Botero 1995)

fy = yield stress of steel and fu= ultimate stress of steel

Table 2 Geometrical uncertainties

Element	Bias factor, λ	Coefficient of variation, V	Reference
Beams caps base	1.01	0.04	(Nowak et al. 2011)
Beams caps height	1.000	0.025	(Nowak et al. 2011)
Column width	1.005	0.04	(Nowak et al. 2011)
Slab thickness	0.00381	8.661	(Ellinwood et al. 1980)

4.2 Nonlinear structural response

The nonlinear structural dynamic response is obtained when plastic hinges (areas of concentrated plasticity) appear. The following conditions are taken into consideration in the analysis: lateral stiffness is provided by cap beams and columns; the bridge deck only transmits dead loads; the failure mechanism is reached when plastic hinges appear either at the base of all columns or at the ends where columns and cap beams join. Ruaumoko 3D program (Carr 2003) is used for obtaining the nonlinear response. The moment-curvature diagram for reinforced concrete is made using both confined concrete (Mander et al. 1988) and the stress-strain model for rebar provided by Rodríguez and Botero (1995). The moment-rotation relationship is estimated with the modified Takeda hysteresis model (see Fig. 5); α and β are related to the stiffness in loading and unloading cycles, taking values between 0.5 - 0.6; the Ramberg-Osgood factor r controls the stiffness loss after rebar yielding, and takes values between $1 \leq r \leq \infty$; k_0 is the initial stiffness, and k_u is the stiffness in the unloading cycle.

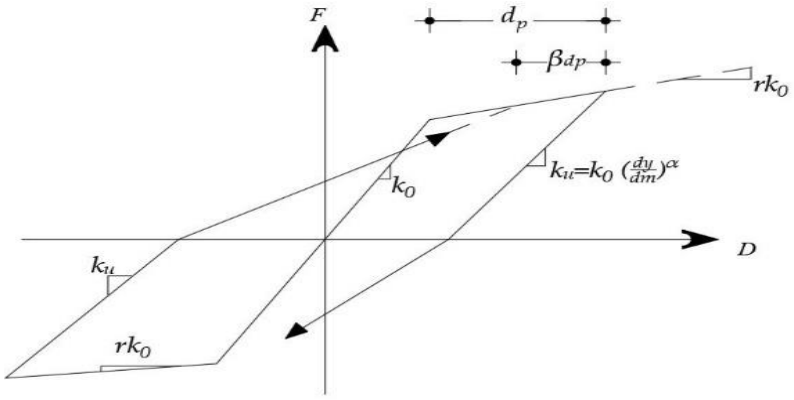

Fig. 5 Modified Takeda Hysteresis Rule

4.3 Seismic records

Seismic loadings occur frequently in Mexico. One of the seismic areas from which subduction ground motions come is the coast of the states of Guerrero, Michoacán and Oaxaca. The devastating seismic loading

266 that hit Mexico City in 1985 originated in such area. Both the design process of new structures and the
267 evaluation of ageing structures in Mexico consider such environmental loads, based on previous experience
268 related to the occurrence of earthquakes and their consequences. Thus, a set of 100 seismic records obtained
269 from the stations "Acapulco Centro Cultural" ACAC and "Acapulco Diana" ACAD are used in this study. Both
270 stations are near the bridge analyzed in this study case. Fig. 6 shows only four recorded ground motions in the
271 area, and Fig. 7 shows the pseudo-acceleration spectrum of the 100 seismic records used.

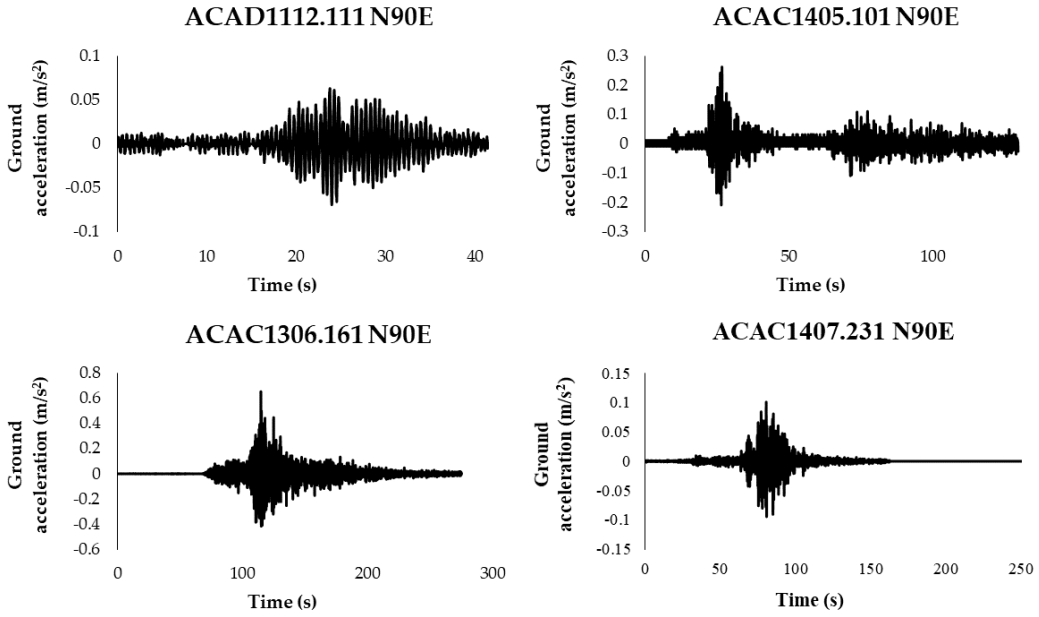

272

273 **Fig. 6** Time history data of four recorded ground motions
274

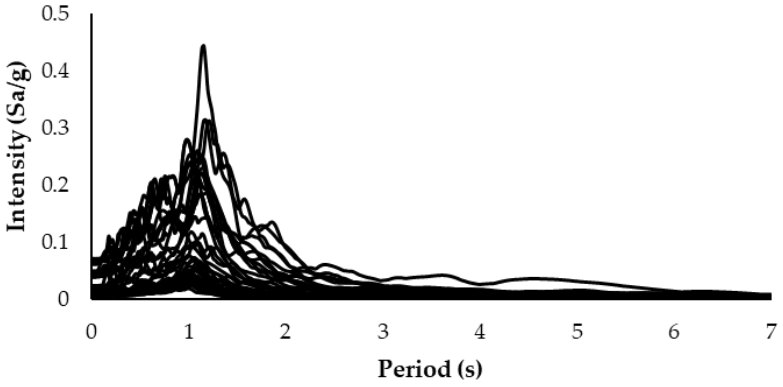

275 **Fig. 7** Response spectra for 100 seismic records

4.4 Corrosion times

The three different stages of corrosion to be evaluated are the starting time of corrosion T_{corr}, corrosion evolution expressed in terms of steel rod reduction at instant $d(t)$, and the instant when concrete cracking starts, Δt_{crack}. In order to estimate T_{corr}, the following values are taken: the mean annual temperature at the site ϕ is 27.8°C; the water – cement ratio w/c is 0.40; C_0 is equal to 0.18% (Castanẽda et al. 1997); C_{cr} is 0.15% (Del Valle et al. 2001); C_i is equal to 0%, and d is the cover thickness, which is equal to 0.05 m. The calculation of the reduced diameter over time $d(t)$ uses the following values: d_0 = 0.0318, c_{corr} = 0.023, and i_{corr} = 0.9. Δt_{crack} is estimated using ρ_{rust} = 3600 kg/m3, ρ_{steel} = 7850 kg/m3, f_t = 0.2456 MPa, and ν_c = 0.2. The starting time of corrosion resulted in 45 years after construction, and the instant of concrete cracking obtained is 57 years after construction. The reduction of the cross-sectional area of reinforcement steel is also estimated for the instants of 75, 100, and 125 years.

4.5 Structural demand over time

The structural demand over time is obtained in accordance with the cumulative damage assessment section. In order to consider uncertainties related to geometric and mechanical properties, fifty bridge models with simulated properties (Sect. 4.1) are built. Uncertainties related to randomness of seismic loadings are considered by means of the construction of one hundred histories of seismic intensities and occurrences. The time instants of 0, 45, 57, 75, 100, and 125 years after the bridge construction are considered; 45 years is the starting time of corrosion; 57 years is the starting time of concrete cracking is; 75 years is the service limit state, according to the AASTHO code (AASTHO, 2012); 100 and 125 years correspond to other times of interest. Fig. 8, which shows the median of demand $\overline{D}_{corr|y,t}$ at different instants, considering the accumulation of damage by both seismic loadings and corrosion, also provides the following information: a) the value of $\overline{D}_{corr|y,t}$ goes up as the instant increases; b) the increment of the median values between the instants of 45

years and 57 years presents important differences due to the appearance of concrete cracking; c) the structural demand increases due to concrete cracking; d) the median value of the demand for 0 years (without damage) at 0.05 Sa/g is equal to 0.0003; for the rest of the subsequent time instants, an initial accumulation of damage as a consequence of seismic sequences and corrosion occurs; e) the median of the demand for instants 45, 57, 75, 100, and 125 years is equal to 0.0005, 0.0009, 0.0018, 0.0023, and 0.0038, respectively, which means that the demand due to both cumulative damage and corrosion for 0.05 Sa/g experiences approximate increments of 170, 279, 556, 721 and 1183%, respectively as well.

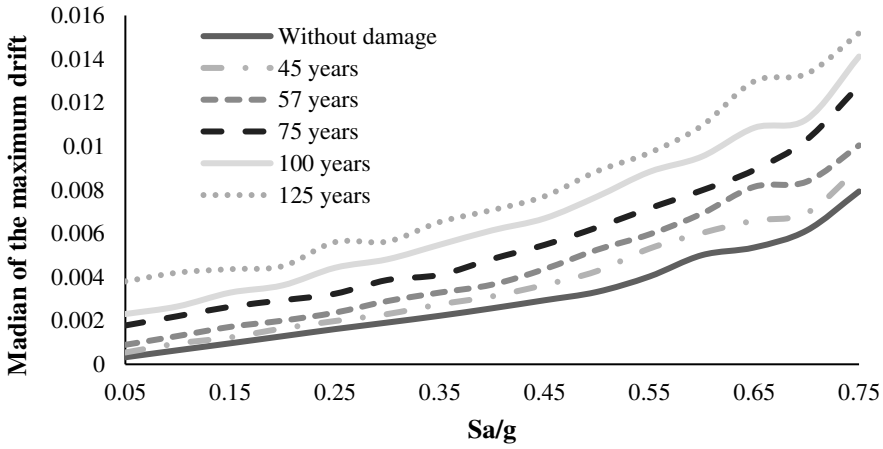

Fig. 8 Median of demand for different time instants

4.6 Fragility curves over time

Fragility curves express the probability that the demand exceeds a pre-stablished threshold. The fragility assessment, considering the accumulation of damage by seismic loads over time, can be calculated as follows (Tolentino et al. 2020):

$$P(D_{corr}(t) \geq d|y,t) = 1 - \Phi\left(\frac{\ln(d) - \ln(\bar{D}_{corr|y,t})}{\sigma_{\ln D_{corr|y,t}}}\right) \quad (19)$$

where $\overline{D}_{corr|y,t}$ represents the median of the demand associated with a certain level of corrosion for an intensity y at a certain instant t; $\sigma_{\ln D_{corr|y,t}}$ is the standard deviation of the demand for an intensity y at a certain instant t, and d represents a pre-established demand threshold. $\overline{D}_{corr|y,t}$ and $\sigma_{\ln D_{corr|y,t}}$ can be estimated as follows:

$$\overline{D}_{corr|y,t} = \exp\left(\frac{\sum_{i=1}^{n} ln\left(Di_{corr|y,t}\right)}{n}\right) \tag{20}$$

$$\sigma_{\ln D_{corr|y,t}} = \left(\frac{\sum_{i=1}^{n}\left(\ln Di_{corr|y,t} - \ln \overline{D}_{|y,t}\right)^2}{n-1}\right)^{\frac{1}{2}} \tag{21}$$

where $Di_{corr|y,\tau}$ is the maximum demanded drift associated with a corrosion damage for an intensity y at time t, and n is the number of cases. Figures 9a-c show the fragility curves over time, calculated with Eq. 19, considering four drift thresholds equal to 0.002, 0.004, 0.006 and 0.012. The value of 0.002 corresponds to the drift threshold design, 0.004 is associated with the service limit state (NTC, 2004), 0.006 is selected as an intermediate threshold, and 0.012 is related to the collapse limit state (NTC, 2004). The insights given by the different parts of Fig. 9 are described below. Fig. 9a shows that the probability of exceeding 0.002 is almost zero for values of Sa/g smaller than 0.10 for 0 and 45 years. On the other hand, the probability of reaching 0.002 is near 1 for values greater than 0.55 Sa/g for all cases. An initial cumulative damage is also noted in the cases of 75, 100 and 125 years for 0.05 Sa/g. Fig. 9b shows that the drift threshold of 0.004 is exceeded for values greater than 0.70 Sa/g, and the probability is close to zero in the cases of 0, 45, and 57 years for intensities not greater than 0.15 Sa/g. Fig. 9c illustrates that the drift of 0.006 is exceeded for values greater than 0.7 Sa/g for the cases of 75, 100, and 125 years. The probability of exceeding 0.006 is close to zero for values smaller than 0.25 Sa/g for 0, 45, and 57 years. For the case of 75 years, the probability is near zero for values of Sa/g less than 0.15. Fig. 9d shows that the maximum probability of exceeding the case of 0.012 results equal to 0.64, which means that there is a certain probability that the structure collapses at 0.75 Sa/g in all instants.

336

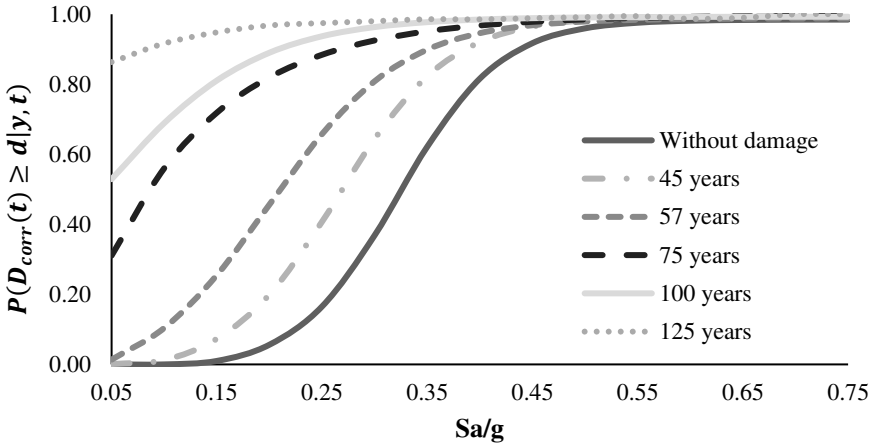
1.00
0.80
0.60
0.40
0.20
0.00
$P(D_{corr}(t) \geq d|y,t)$
0.05
0.15
0.25
0.35
0.45
0.55
0.65
0.75
Sa/g
Without damage
45 years
57 years
75 years
100 years
125 years

(**a**)

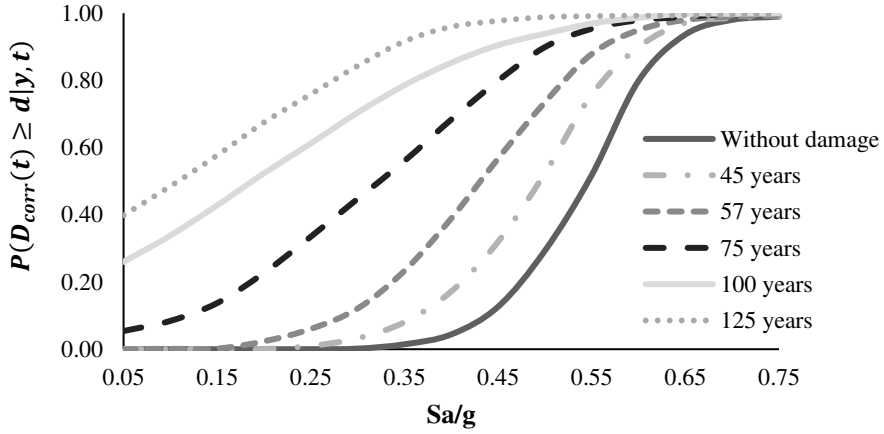
1.00
0.80
0.60
0.40
0.20
0.00
$P(D_{corr}(t) \geq d|y,t)$
0.05
0.15
0.25
0.35
0.45
0.55
0.65
0.75
Sa/g
Without damage
45 years
57 years
75 years
100 years
125 years

(**b**)

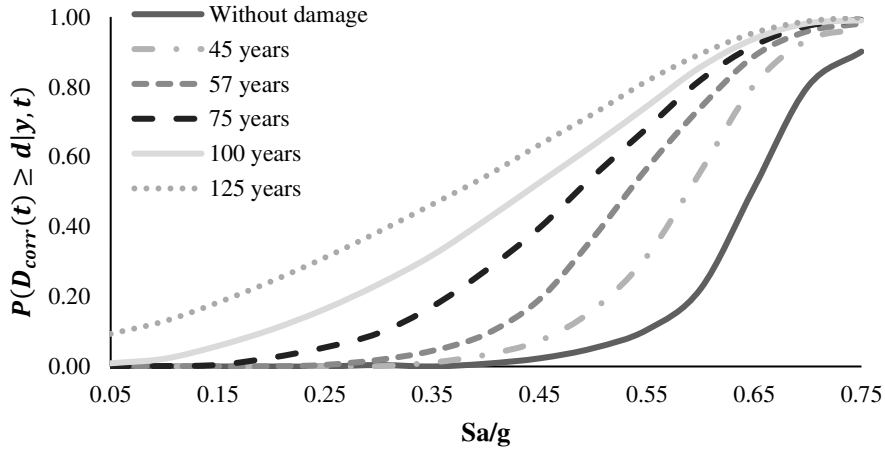
1.00
0.80
0.60
0.40
0.20
0.00
$P(D_{corr}(t) \geq d|y,t)$
0.05
0.15
0.25
0.35
0.45
0.55
0.65
0.75
Sa/g
Without damage
45 years
57 years
75 years
100 years
125 years

(**c**)

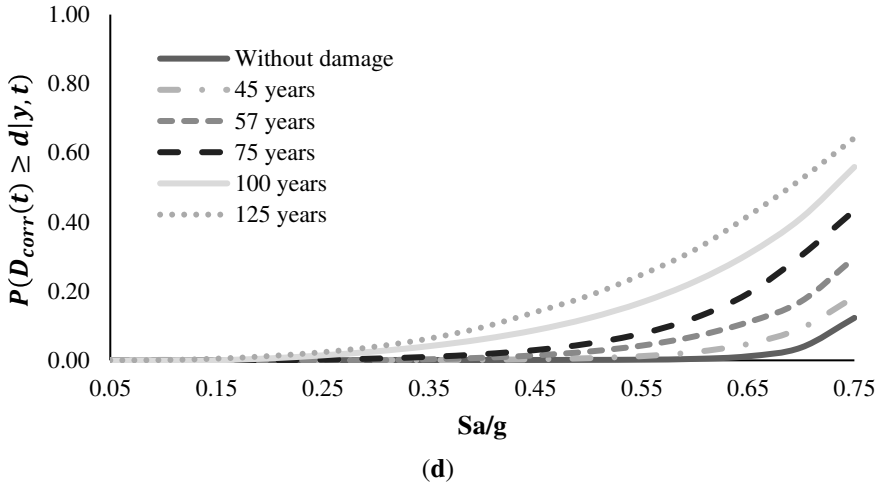

(**d**)

Fig. 9 Fragility curves over time considering 0, 45, 57, 75, 100 and 125 years: (a) 0.002, (b) 0.004, (c) 0.006, (d) 0.012

4.7 Demand hazard curves considering cumulative damage

Demand hazard curves indicate the number of times that a certain drift threshold is exceeded per unit of time. They also give information for decision-making processes when the limit state under consideration is reached. Figure 10 illustrates the demand hazard curves (Eq. 3) for instants 0, 45, 57, 75, 100, and 125 years. Such curves are made considering the maximum drift at the deck. Fig. 10 also shows the following: i) the exceedance drift rate increases when the cumulative damage over time is considered; ii) for the case of design drift (0.002), exceedance rates of 0.015, 0.018, 0.022, 0.031, 0.039, and 0.049 result for the cases of 0, 45, 57, 75, 100 and 125 years, respectively; iii) the demand exceedance rate grows as the cumulative damage increases over time; iv) there are important differences between 57 and 75 years due to the changes in the evolution of corrosion; v) at 57 years, cracking occurs, and the demand hazard curve in 75 years is obtained considering the cracking, the reduction of diameter in steel reinforcement, and seismic loadings, yielding a result with a difference of 140% for the case of 0.002; vi) the differences of exceedance demand rates for the cases of 100 and 125 years are mainly due to the increment of the occurrences of seismic loadings. Such differences represent increments of 128 and 159% for 100 and 125 years with respect to 75 years, for d equal to 0.002.

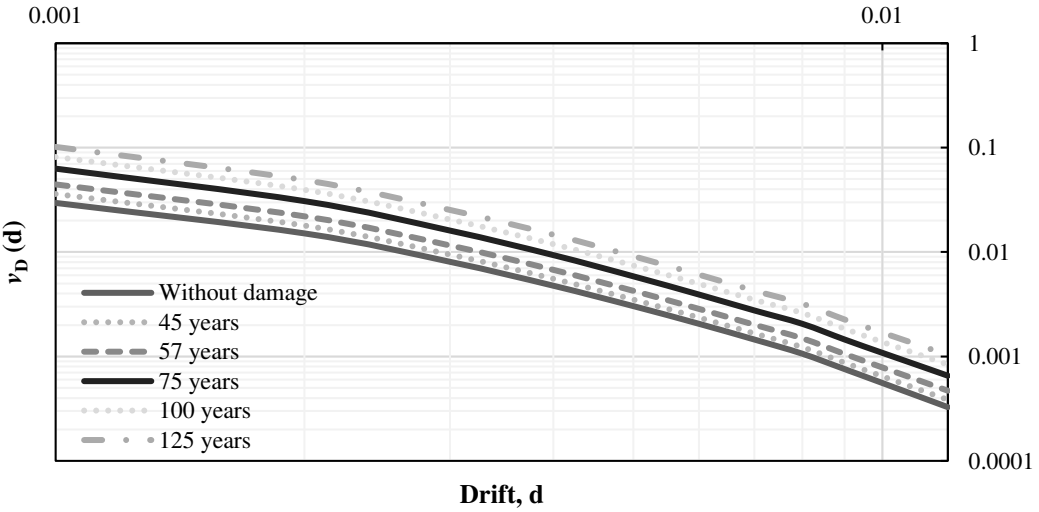

353

354 **Fig. 10** Demand hazard curves for thresholds of 0, 45, 57, 75, 100 and 125 years
355

356 ## 5. Conclusions

357 An approach to obtain demand hazard curves that considers both cumulative damage caused by
358 corrosion and seismic sequences was proposed; cumulative damage over time was obtained considering any
359 repair action at any instant; uncertainties related to mechanical properties, geometric properties, and seismic
360 loadings were considered; structural damage over time was expressed in terms of global drift. The expression
361 proposed to obtain demand hazard curves is generalized, and can be used in other types of structures with
362 different loadings.

363 The approach was illustrated in a continuous bridge designed to comply with a value of drift equal to
364 0.002. Different instants of corrosion and simulation of seismic occurrences were considered to estimate the
365 possible cumulative damage over time. In order to obtain demand hazard curves, different fragility curves were
366 obtained, based on instants of 0, 45, 57, 75, 100, and 125 years, considering drift thresholds of 0.002, 0.004,
367 0.006 and 0.012. Cumulative damage due to both seismic sequences and corrosion leads the structure to present
368 high probabilities of exceeding all drift thresholds for the intensities under study. According to the

recommendations given by AASHTO code, the service life of bridges must be guaranteed up to 75 years. The probability that the drift value of 0.004 (service limit state) is exceeded at 75 years, in accordance with the IMT code, is low for values less than 0.2 Sa/g; such limit state is exceeded for values greater than 0.65 Sa/g. Therefore, reinforced concrete bridges could be designed considering a pre-established design drift threshold, because higher intensities are needed to exceed the service limit state.

Demand hazard curves were determined for different instants, considering drift thresholds between 0.001 and 0.012. For the design drift threshold of 0.002, demand exceedance rates equal to 0.0151, 0.0179, 0.0220, 0.0308, 0.0394, and 0.0489 were obtained for instants 0, 45, 57, 75, 100, and 125 years, respectively. On the other hand, values of demand exceedance rates for the case of 0.004 result equal to 0.00476, 0.00555, 0.00676, 0.00935, 0.01191, and 0.01467 for instants 0, 45, 57, 75, 100, and 125 years, respectively. Such values represent differences of 116.51%, 141.94%, 196.49%, 250.19%, and 308.16% between 0 to 125 years. If the structure were designed based on a pre-established demand exceedance rate, the final design of the structure would change, whether the effects of cumulative damage were taken into account or not.

The proposed approach allows evaluating the conditions in which a structure is after it has been subjected to both seismic sequences and deterioration by corrosion. The information provided by such evaluation is helpful in the decision-making process during the design of new structures. If the drift that represents the exceedance of a given limit state is known, the demand hazard curves will indicate the reserves of structural strength that the structure has in a certain instant. Moreover, the approach presented also provides useful information on the structural performance over time, which can be taken as the basis for maintenance and inspection plans with the aim of preserving the structure with adequate reliability levels.

Acknowledgements: The first author would like to thank both Universidad Autónoma Metropolitana (UAM) and the Consejo Nacional de Ciencia y Tecnología (CONACyT) for the support provided through the Ciencia

básica Project CB 2017-2018 A1-S-8700. The second and third authors would like to thank both CONACyT and UAM for their economical support during their Ph.D. studies.

References

AASHTO (2012) Standard specifications for highway bridges. American Association of State Highway and Transportation Officials. Washington DC, USA

Andrade C, Alonso C, Molina, FJ (1993) Cover cracking as a function of bar corrosion: Part I-Experimental test. Mater Struct 26:453–464. https://doi.org/10.1007/BF02472805

Bertolini L (2008) Steel corrosion and service life of reinforced concrete structures. Struct Infrastruct Eng 4:123–137. https://doi.org/10.1080/15732470601155490

Cabrera JG (1996) Deterioration of concrete due to reinforcement steel corrosion. Cem Concr Compos 18:47–59. https://doi.org/10.1016/0958-9465(95)00043-7

Carr AJ (2003) RUAUMOKO 3D Volume 3: User manual for the 3-Dimensional version. Christchurch, University of Canterbury, New Zealand

Castanĕda H, Castro P, González C, Genescá J (1997) Mathematical model for chloride diffusion in reinforced concrete structures at Yucatan Peninsula, México. Rev de Metal 33:387–392. https://doi.org/10.3989/revmetalm.1997.v33.i6.834

Choi E, Jeon JC (2003) Seismic fragility of typical bridges in moderate seismic zone. KSCE J Civ Eng 7:41–51. https://doi.org/10.1007/bf02841989

Cornell CA, Jalayer F, Hamburger RO, Foutch DA (2002) Probabilistic Basis for 2000 SAC Federal Emergency Management Agency Steel Moment Frame Guidelines. J Struct Eng 128:526–533.

411 https://doi.org/10.1061/(ASCE)0733-9445(2002)128:4(526)

412 Cui S, Guo C, Su J, Cui E, Liu P (2019) Seismic fragility and risk assessment of high-speed railway continuous-
413 girder bridge under track constraint effect. Bull Earthq Eng 17:1639–1665.
414 https://doi.org/10.1007/s10518-018-0491-9

415 Del Valle A, Pérez T, Martínez M (2001) El fenómeno de la corrosión en estructuras de concreto reforzado,
416 Instituto Mexicano del Transporte, Publicación No.182 (in Spanish)

417 Ellinwood BR, Galambos TV, McGregor JG, Cornell CA (1980) Development of a probability based load
418 criterion for american national standard, National bureau of standards special publication 577

419 Fick A (1855) Ueber Diffusion. Ann Phys 170:59–86. https://doi.org/10.1002/andp.18551700105

420 Gavabar SG, Alembagheri M (2018) Structural demand hazard analysis of jointed gravity dam in view of
421 earthquake uncertainty. KSCE J Civ Eng 22, 3972–3979. https://doi.org/10.1007/s12205-018-1009-3

422 IMT (2001) Proyecto de puentes y estructuras. Instituto Mexicano del Transporte. Queretaro, Mexico (in
423 Spanish)

424 Jaffer SJ, Hansson CM (2009) Chloride-induced corrosion products of steel in cracked-concrete subjected to
425 different loading conditions. Cem Concr Res 39:116–125.
426 https://doi.org/10.1016/j.cemconres.2008.11.001

427 Kim SH, Feng MQ (2003) Fragility analysis of bridges under ground motion with spatial variation. Int J Non
428 Linear Mech 38:705–721. https://doi.org/10.1016/S0020-7462(01)00128-7

429 Liu Y, Weyers RE, (1998) Modeling the time-to-corrosion cracking in chloride contaminated reinforced
430 concrete structures. ACI Mater J 95:675–681. https://doi.org/10.14359/410

Liu XX, Wu ZY, Liang F (2016) Multidimensional performance limit state for probabilistic seismic demand analysis. Bull Earthq Eng 14:3389–3408. https://doi.org/10.1007/s10518-016-0013-6

Mackie K, Stojadinović B (2001) Probabilistic seismic demand model for California highway bridges. J Bridge Eng 6:468–481. https://doi.org/10.1061/(ASCE)1084-0702(2001)6:6(468)

Maleki M, Ahmady Jazany, R., Ghobadi MS (2019) Probabilistic seismic assessment of SMFs with drilled flange connections subjected to near-field ground motions. Int J Steel Struct 19:224–240. https://doi.org/10.1007/s13296-018-0112-0

Mander JB, Priestley MJN, Park R (1988) Theoretical stress-strain model for confined concrete. J Struct Eng 114:1804–1826. https://doi.org/10.1061/(ASCE)0733-9445(1988)114:8(1804)

Mangat PS, Molloy BT (1994) Prediction of long term chloride concentration in concrete. Mater Struct 27: 338–346. https://doi.org/10.1007/BF02473426

Melchers RE, Beck AT (2018) Structural reliability analysis and prediction. JohnWiley & Sons Ltd., Hoboken, NJ, USA

Nowak AS, Rakoczy AM, Szeliga EK (2011) Revised statistical resistance models for R/C structural components. ACI Symp Publ 284:61–76. https://doi.org/10.14359/51683801

NTC (2004) Normas técnicas complementarias del reglamento de construcción de la Ciudad de México. Gaceta Oficial. Mexico City, Mexico (in Spanish)

Padgett JE, DesRoches R (2008) Methodology for the development of analytical fragility curves for retrofitted bridges. Earthq Eng Struct 37:1157–1174

Panchireddi B, Ghosh J (2019) Cumulative vulnerability assessment of highway bridges considering corrosion

deterioration and repeated earthquake events. Bull Earthq Eng 17:1603–1638. https://doi.org/10.1007/s10518-018-0509-3

Papakonstantinou KG, Shinozuka M (2013) Probabilistic model for steel corrosion in reinforced concrete structures of large dimensions considering crack effects. Eng Struct 57:306–326. https://doi.org/10.1016/j.engstruct.2013.06.038

Rodríguez M, Botero J (1995) Comportamiento sísmico de estructuras considerando propiedades mecánicas de aceros de refuerzo mexicanos. Rev Ing Sísmica 49:39–50. https://doi.org/10.18867/ris.49.268

Schwerdtfeger WJ, Romanoff M (1972) NBS papers on underground corrosion of steel piling 1962-1971: corrosion of steel pilings in soils, corrosion evaluation of steel test piles exposed to permafrost soils, performance of steel pilings in soils, polarization measurements as related to corrosion underground stel piling

Thoft-Christensen P (2000) Stochastic modeling of the crack initiation time for reinforced concrete structures. Structures Congress 2000 1–8. https://doi.org/10.1061/40492(2000)157

Thoft-Christensen P (2002) Corrosion and cracking of reinforced concrete. Third IABMAS workshop on life-cycle cost analysis and design of civil infrastructures systems 26–36. https://doi.org/10.1061/40707(240)4

Thoft-Christensen P (2003) Stochastic modelling of the diffusion coefficient for concrete. Aalborg University's Research Portal R0204, 151–159.

Tolentino D, Márquez-Domínguez S, Gaxiola-Camacho JR (2020) Fragility assessment of bridges considering cumulative damage caused by seismic loading. KSCE J Civ Eng 24:551–560. https://doi.org/10.1007/s12205-020-0659-0

Wang Q, Wu Z, Liu S (2018) Multivariate probabilistic seismic demand model for the bridge multidimensional fragility analysis. KSCE J Civ Eng 22:3443–3451. https://doi.org/10.1007/s12205-018-0414-y

Wang Q, Wu Z, Liu S (2012) Seismic fragility analysis of highway bridges considering multi-dimensional performance limit state. Earthq Eng Eng Vib 11:185–193. https://doi.org/10.1007/s11803-012-0109-1

Zaker Esteghamati M, Farzampour A (2020) Probabilistic seismic performance and loss evaluation of a multi-story steel building equipped with butterfly-shaped fuses. J Constr Steel Res 172:106187. https://doi.org/10.1016/j.jcsr.2020.106187